ESTIMATING THE PERMEABILITY OF CARBONATE ROCKS USING IMAGE ANALYSIS AND EFFECTIVE MEDIUM THEORY

M. Jurgawczynski[1], R. W. Zimmerman[1], and X. D. Jing[2]
[1]Dept. of Earth Science and Engineering, Imperial College, London, SW7 2AZ, U.K.
[2]Shell International Exploration and Production, 2280 AB Rijswijk, The Netherlands

This paper was prepared for presentation at the International Symposium of the Society of Core Analysts held in Abu Dhabi, UAE, 5-9 October, 2004

ABSTRACT

A methodology was recently developed at Imperial College to estimate the permeability of sedimentary rocks from two-dimensional pore images [1]. The only data required from the images are the areas and perimeters of the individual pores. From this information, the hydraulic conductivities of the individual pores are estimated. The overall permeability of the rock is then estimated using effective medium theory. In contrast to methods that require reconstruction of the 3-dimensional pore structure and the solution of network flow equations, our approach requires minimal calculation. The procedure was tested on scanning-electron micrograph (SEM) images of more than twenty North Sea reservoir cores, and the permeability was generally predicted within a factor of two.

This methodology is currently being applied to carbonate rocks, which generally have more complex and heterogeneous pore structures. Despite this difference, preliminary work on several carbonates rocks have given encouraging results, with the predictions again typically being within factor of two of the measured permeabilities, for rocks that do not contain large vugs that are unconnected to the main pore network. Nevertheless, we are currently investigating the extent to which the methodology will need to be modified for carbonates. For example, in sandstones it was found to suffice to assume that the pore network has a co-ordination number of six. This may need to be modified for different types of carbonates. In addition, a method needs to be developed to be able to identify isolated vugs, and remove them from the permeability calculation.

Aside from giving insight into the influence of pore structure on permeability, the method has potential applications for making permeability predictions using drill cuttings, in situations where it is not possible to recover intact core. Another possible application is to use downhole borehole imaging technology to provide an image with the appropriate resolution, thereby allowing permeability estimation without the need for core samples.

INTRODUCTION

The ability to estimate the permeability of a reservoir rock from other more readily measurable parameters would be of great value to the oil industry. Empirical permeability models such as the Kozeny-Carman equation [2] make use of the porosity and a specific surface parameter. Although simple to implement, the Kozeny-Carman equation is often found to be insufficiently accurate for reservoir characterization purposes. The Katz-Thomson equation [3] can yield accurate estimations of the permeability, using the porosity and the electrical formation factor. However, the requirement of having a measured value of the electrical formation factor is clearly a disadvantage of this method.

At the other extreme of complexity lie those models that attempt to reconstruct the pore space of a rock, and then numerically solve the Navier-Stokes equations in the pore space. Adler *et al*. [4] reconstructed the pore space of Fontainebleau sandstones from thin sections and then solved the Navier-Stokes equations using a finite-difference scheme to yield the permeability. Spanne *et al.* [5], and later Ferréol and Rothman [6], used X-ray microtomography to reconstruct the pore structure of a Fontainebleau sandstone, from which the permeability was calculated numerically, in the latter case using the lattice-Boltzmann method. Such approaches are capable of good accuracy, but at the expense of extensive data collection and computation.

We have been developing a method for predicting permeability from two-dimensional images of the pore space, without requiring any computationally intensive procedures. The hydraulic conductivities of the individual pores are estimated from their areas and perimeters using the hydraulic radius approximation. Stereological correction factors are applied to determine the true cross-sectional shapes from the images, and to determine the true number density of pores per unit area. A constriction factor accounts for the variation of the cross-sectional area along the tube length. The pores are assumed to be arranged in a cubic lattice, after which the effective-medium theory of Kirkpatrick [7] is used to estimate the effective conductance of the pores. Finally, the permeability is estimated from the effective pore conductance and the number density of pores.

This methodology has previously been applied [1] to several reservoir sandstones from the North Sea, and a few outcrop sandstones, having permeabilities in the range of 20-1400 mD. The permeability estimates were almost always within a factor of two of the values measured in the laboratory, with an average error, in absolute value, of less than 50%. In the present paper we briefly review the procedure as developed for sandstones, and then describe its application to some carbonate rocks. Finally, we discuss possible refinements to the procedure that may be necessary for carbonates.

CONDUCTANCE OF INDIVIDUAL PORES

Effect of pore shape

Consider an individual pore of length L, with a pressure drop ΔP along its length. The volumetric flowrate Q through this pore can be written as $Q = G\Delta P / \mu L$, where μ is the fluid viscosity and G is the "hydraulic conductance". First, imagine that we can idealize an individual pore as a prismatic tube having a uniform, although possibly irregular, cross-section. If the cross section were circular, with radius r, the "hydraulic conductance" would be given by $G = \pi r^4 / 8$, according to Poiseuille's law. Written in terms of the area A and perimeter Γ of the pore, this result is $G = A^3 / 2\Gamma^2$. According to the hydraulic radius approximation, this result can be used for non-circular cross sections. By comparison with boundary element solutions to the flow equations in a pores taken from images of Massilon and Berea sandstones, Sisavath *et al*. [8] found that this approximation is, on average, accurate to better than 20%.

Effect of converging-diverging cross-section

The hydraulic-radius approximation is intended to apply to a cylindrical pore with uniform cross-section. However, the cross-section of rock pore typically varies along the length of the pore. By integrating the Poiseuille equation along the length of a pore, it can be shown that $G = \pi < r^{-4} >^{-1} / 8$, where $< \cdot >$ denotes an average taken over the length of the tube. If we estimate the radius of such a tube based on a single thin section of rock, however, we would be estimating the mean value of the radius, $< r >$, and would predict that $G = \pi < r >^4 / 8$. Hence, the actual conductance will be less than that estimated from the mean radius by a factor of

$$f \equiv \frac{G(actual)}{G(predicted)} = \frac{< r^{-4} >^{-1}}{< r >^4} \leq 1, \tag{1}$$

where f can be referred to as the *hydraulic constriction factor*.

For a pore whose radius varies as a sinusoidal function of the position along the pore, the constriction factor can be calculated to be [1]

$$f(\text{sinusoidal}) = \frac{256\rho^{7/2}}{(1+\rho)^4(5\rho^3 + 3\rho^2 + 3\rho + 5)}, \tag{2}$$

where $\rho = r_{\min} / r_{\max}$. The constriction factors calculated for sawtooth or step-function variations of radius are quite similar to (2), except for values of ρ less than about 0.20, which is probably an unrealistically small value.

Lock *et al*. [1] did not investigate the problem of estimating $r_{\min} / r_{\max}$ from two-dimensional images. Instead, based on various pieces of evidence gleaned from the literature, they adopted a value of 0.43 for sandstones, in which case equation (2) gives a hydraulic constriction factor of 0.44.

Stereological correction for area and perimeter

The areas and perimeters of the individual pores, as measured from any 2D image, will in general be *larger* than the actual values for the pore cross-sections. For example, consider a cylindrical pore of radius r. In general, the plane of the image will intersect this pore at some arbitrary angle θ relative to the pore axis, and so the pore will appear as an ellipse with a semi-minor axis of r, but a semi-major axis of $r/\cos\theta$. Hence, the area and perimeter of the image would consequently be larger than the actual area and perimeter of the pore, and so the estimated hydraulic conductance will be greater than the actual value. An approximate stereological correction factor that converts the "measured" values of the hydraulic conductance into "actual" values can be found by averaging the overestimation in the conductance G over all possible angles, assuming that the pores are randomly oriented with respect to the plane of the image. The result [1] of this calculation is that the pore conductances estimated from the image must be multiplied by 0.375 to arrive at the "true" conductance of the pore.

Stereological correction for number density

Consideration must also be made of the overestimation in the areal number density of pores that occurs as a consequence of taking an arbitrary two-dimensional slice that probably does not lie in a plane perpendicular to a lattice direction. If we again consider the idealization of pore microstructure by a hypothetical cubic lattice, then a slice taken perpendicular to a given lattice direction will only intersect those pores that lie along that direction. If, however, the slicing plane is not normal to the lattice direction, it will also intersect some pores that are orthogonal to that first lattice direction. Evaluation of this effect [1] leads to the conclusion that the apparent number density of pores (*i.e.*, pores per unit area of image) must be divided by 1.47 to yield the actual density of pores that are oriented in a given lattice direction. An analogous calculation for a rock containing pores having a random distribution of orientations gives an identical result.

NETWORK MODELS

Network models have been used to study the transport properties of porous media since the pioneering work of Fatt [9] in the 1950s. Early studies used idealized pore shapes and hypothetical pore-size distributions to gain insight into the physics of pore-scale flow processes, and to study the influence of parameters such as co-ordination number and porosity. More recently, there has been a trend towards the use of rock-specific pore geometry data, as obtained from methods such as NMR imaging [10] or mercury intrusion porosimetry [11], in attempts to predict the transport properties of a given rock sample. A critical review of recent work on pore network models, with an emphasis on multi-phase flow, has been given by Blunt [12].

We assume that the pore space can be represented by a network of pore tubes, connected to each other at (volumeless) nodes. If the values of all of the conductances were known exactly, and the topology of the network was also known, evaluation of the overall macroscopic conductance of the network would require the solution of the large system

of linear equations that arises by applying the equation $Q = G\Delta P / \mu L$ to each tube, and invoking the fact that the sum of the fluxes into each node must be zero in order to conserve mass. An alternative to an "exact" network calculation is the effective medium approximation (EMA) of Kirkpatrick [7], in which each conductor G_i in the network is replaced by a conductor having some effective value G_{eff}, which is found by solving the following implicit equation for G_{eff}:

$$\sum_{i=1}^{N} \frac{G_{eff} - G_i}{(z/2-1)G_{eff} + G_i} = 0, \tag{3}$$

where the co-ordination number *z* represents the number of conductors that meet at each node, and the summation is taken over each individual conductor in the network. In our work we set *z* = 6, which corresponds to a cubic lattice. Other researchers [13-17] have estimated the mean co-ordination number for sandstones to be in the range of 3-8.

A discussion of the accuracy of the effective medium approximation has been given by Koplik [13] and David *et al*. [14], for various idealized distributions. Lock *et al.* [18] compared the EMA predictions with exact solutions of the network equations, and found errors of less than 2-3%.

The last step involves computing the permeability of the continuous medium from the effective conductance of the individual conductors. Imagine a plane that slices the lattice perpendicular to one of the lattice directions, containing *N* pores in a region of total area *A*. The total flowrate through this region is given by $Q = NG_{eff}\Delta P / \mu L$. Equating this to the flux as given by Darcy's law, $Q = kA\Delta P / \mu L$, then yields

$$k = NG_{eff} / A. \tag{4}$$

IMAGE ANALYSIS OF PORE STRUCTURE

We start with two-dimensional cross-sectional images of the rock. Regardless of their origin, the images must be converted into digitized grey-scale images in which the pore space is generally distinguished from the various minerals by having higher grey-scale values. The images are then thresholded to yield binary images in which the pores are black and the mineral grains are white. We have performed this analysis using the "Scion Image for Windows" image analysis package, Version Image Beta1a, 1997. Details of the image analysis procedure can be found in [1].

We have found that this thresholding procedure leads to the identification of a large number of very small "pores" that are probably either unconnected to the conducting pore space, or which are merely artifacts of the digitization process. We remove these features by applying a cutoff that deletes those features whose areas are < 1% of the area of the largest pore in the image.

The issue of pixel size is of importance in this type of analysis. Use of a pixel size that is too large, relative to the pore sizes, will lead to the loss of fine-scale pore features, and consequent inaccuracy in the estimation of the hydraulic conductances. On the other hand, use of a pixel size that is "too small" will capture small-scale pore roughness features that do not influence the hydraulic transmissivity, and so will lead to a perimeter term in the hydraulic conductance equation that is too large, thereby underestimating the conductance. Berryman and Blair [2] proposed that the pixel size be approximately 1% of the average pore diameter. Sisavath *et al.* [8], concluded that the ratio of pixel/pore size could be as large at 10% before any accuracy is lost.

Sensitivity to magnification has been studied in [2] and [8]. If the magnification is too low, important details of the pore structure are lost, whereas if it is too high, the image captures small-scale pore roughness that actually has no influence on the flow. A related issue is the total area of view that is required to yield a sufficiently large sample of pores. For sandstones, we have found that images as small as 5-6 pores in each direction may be sufficient to allow us to predict core-scale permeabilities. But some carbonates are quite heterogeneous, and the so-called "representative elementary volume" may be much larger than our millimetre-scale images. These are difficult and long-standing issues that we are continuing to investigate.

ANALYSIS OF CARBONATE SAMPLES

We have taken the methodology developed in [1] for sandstones, and applied it to a set of carbonate rocks having permeabilities in the range of 0.5 to 25 mD. In each case we start with a back-scattered electron (BSE) micrograph image of the rock. In this early stage of our investigations, we have decided to test the method "as is", without making any modifications to account for any fundamental differences between sandstones and carbonates, as regards to pore structure. Specifically, we have been using the same constriction factor (which in principle depends on the ratio of minimum to maximum pore radius for a given pore), and have again assumed a mean co-ordination number of 6.

Sample A (Fig. 1)

This is a poorly-sorted peloidal grainstone. Porosity is shown here in black as usual, microporosity is shown in grey grades. Macroporosity is rare within this sample, which is instead characterized by diffuse microporosity. When looking at the sample at higher resolutions (×2000), we find that, in some areas, most of the original primary intraparticle porosity has been cemented by calcite.

The area of view of this is 337×193 μm^2, with a total of 600×343 pixels. After analysing the sample with Scion Image, we find 1403 "pore" features, most of which are eventually discarded as part of the areal thresholding process. Therefore, the number of pores effectively used to find the overall conductance is 426. The permeability predicted by our approach, 2.7 mD, is within 8% of the measured value of 2.5 mD.

Sample D (Fig. 2)
This is clearly a carbonate with separate vuggy pores and macroporosity. Some of the pores are up to 0.8 mm in diameter; these are probably moldic pores. We can also notice the scale of the sample, which is much larger than other samples presented here. However, there also is microporosity, which gives us a very heterogeneous sample.

The area of view of this is 5010×2965 μm^2, for a pixel resolution of 700×414 pixels. The number of "pores" initially identified in the image analysis procedure is 1028 pores, whereas only 86 survive the thresholding procedure. The predicted permeability of 3002 mD is two orders of magnitude larger than the measured value of 25 mD.

Sample E (Fig. 3)
This sample is a back scattered image of a very poorly-sorted peloidal grainstone. One can immediately appreciate the heterogeneity of the pore system, which is ranging from interparticle micro-pores to intraparticle macro-pores. When looking at the sample at higher resolution (×2000), we notice tight calcite crystals arrangement that cause the micro-pore system to be fairly isolated in certain parts of the sample. Also, there are signs of possible re-crystallization processes.

The area of view of this image is 1873×1070 μm^2, for a pixel resolution of 700×414 pixels. The initial number of pore-like features identified with Scion Image is 822, of which 162 survive the areal thresholding process. In this case the estimated permeability of 12.5 mD is very close to the measured value of 13 mD.

Sample F (Fig. 4)
This sample is a poorly-sorted peloidal-bioclastic grainstone. The image shown below illustrates a high magnification view on an area dominated by peloidal material (porous areas). Structured grains are probably a diagenetic product. When looking at higher resolution (×2000), we can see that peloids have been leached away but intergranular cements are preserved - large calcite crystals with straight edges. Pores are mostly present in the leached peloids, whereas very little porosity is seen within the cements.

The area of view of this is 187×107 μm^2, for a pixel resolution of 700×400 pixels. Scion Image identifies 1904 "pores", of which 617 remain after areal thresholding. The predicted permeability, 3.7 mD, is within a factor of 2 of the measured value of 1.9 mD.

Discussion of Results
The results for the four samples are summarized in Table 1. The porosity values listed are those calculated from the images, not those measured in the laboratory. In three cases (A, E and F) the method works just as well as it did for sandstones in [1]. The permeability is, in these three cases, predicted within about a factor of two.

Table 1: Results for some carbonate samples.

Sample	Porosity	No. of Pores	k_{pred} (mD)	k_{meas} (mD)
A	4.3%	426	2.7	2.5
D	13.7%	86	3002	25.0
E	4.3%	162	12.5	13.0
F	14.7%	617	3.7	1.9

In the case of sample, D, the permeability is overpredicted by about two orders of magnitude. Unsurprisingly, it is one the sample that presents the most heterogeneity, namely a combination of macroporosity (vuggy pores up to 0.8 mm) as well as microporosity. This heterogeneity can be quantified by examining the ratio of the largest to smallest pore (by area) identified in the image analysis process. This ratio is about 2000 for sample D, 125 for sample A, 200 for sample E, and 60 for sample F. However, it is clear that an objective method is needed to identify non-connected vugs, so that they can be excluded, with some justification, from the calculation of the effective pore conductivity. We are investigating the use of statistical methods to identify those pores that are clearly not part of the same population as the main pore network.

Based on our analysis of a relatively small number of samples, including a few not described in this paper, it seems that the method either works quite well, or not very well at all. The fact that the method often makes predictions that are probably within the error bars of the laboratory permeability measurements would seem to argue that the method developed in [1] to determine the permeability from the geometry of the individual pores that are part of the conducting network, does not require any fine-tuning. What does seem to be needed is a method for identifying *a priori* those pores that do not form part of the interconnected pore network. If the samples are impregnated with epoxy before sectioning and imaging, the non-connected pores could be identified by the lack of epoxy. As mentioned above, we are also investigating statistical methods to identify these pores that are "outliers" of the main population.

ACKNOWLEDGEMENTS

We thank Shell International E&P Technology for sponsoring M. Jurgawczynski's research at Imperial College London, and for their kind permission to publish this paper.

REFERENCES

1. Lock P. A., X. D. Jing, R. W. Zimmerman, and E. M. Schlueter, Predicting the permeability of sandstone from image analysis of pore structure, *J. Appl. Phys*., (2002) 92, 6311-19.

2. Berryman, J. G. and S. C. Blair, Kozeny-Carman relations and image processing methods for estimating Darcy's constant, *J. Appl. Phys*., (1987) **62**, 2221-28.

3. Katz, A. J. and A. H. Thompson, Quantitative prediction of permeability in porous rock, *Phys. Rev. B*, (1986) **34**, 8179-81.

4. Adler, P. M., C. G. Jacquin, and J. A. Quiblier, Flow in simulated porous media, *Int. J. Multiphase Flow*, (1990) **16**, 691-712.
5. Spanne, P., J.-F. Thovert, C. J. Jacquin, W. B. Lindquist, K. W. Jones, and P. M. Adler, Synchrotron computed tomography of porous media – topology and transports, *Phys. Rev. Letts.,* (1994) **73**, 2001-04.
6. Ferréol, B. and D. H. Rothman, Lattice-Boltzmann simulations of flow through Fontainebleau sandstone, *Transp. Porous Media,* (1995) **20**, 3-20.
7. Kirkpatrick, S., Percolation and conduction, *Rev. Mod. Phys*., (1973) **45**, 574-88.
8. Sisavath, S., X. D. Jing, and R. W. Zimmerman, Laminar flow through irregularly-shaped pores in sedimentary rocks, *Transp. Porous Media,* (2001) **45**, 41-62.
9. Fatt, I., The network model of porous media. I. Capillary pressure characteristics, *Trans. AIME*, (1956) **207**, 144-59.
10. Damion, R. A., K. J. Packer, K. S. Sorbie, and S. R. McDougall, Pore-scale network modelling of flow propagators derived from pulsed magnetic field gradient spin echo NMR measurements in porous media, *Chem. Eng. Sci*., (2000) **55**, 5981-98.
11. Matthews, G. P., A. K. Moss, and C. J. Ridgway, The effects of correlated networks on mercury intrusion simulations and permeabilities of sandstone and other porous-media, *Powder Tech*., (1995) **83**, 61-77.
12. Blunt, M. J., Flow in porous media - pore-network models and multiphase flow, *Curr. Opin. Colloid Interface Sci*., (2001) **6**, 197-207.
13. Koplik, J., On the effective medium theory of random linear networks, *J. Phys. C*, (1981), **14**, 4821-37.
14. David, C., Y. Gueguen, and G. Pampoukis, Effective medium theory and network theory applied to the transport properties of rock, *J. Geophys. Res*., (1990) **95**, 6993-7005.
15. Koplik, J., Creeping flow in two-dimensional networks, *J. Fluid Mech*., (1982) **119**, 219-47.
16. Doyen, P., Permeability, conductivity and pore geometry of sandstone, *J. Geophys. Res*., (1988) **93**, 7729-40.
17. Jerauld, G. R., and S. J. Salter, The effect of pore structure on hysteresis in relative permeability and capillary pressure – pore-level modeling, *Transp. Porous Media*, (1990) **5**, 103-51.
18. Lock, P. A., X. D. Jing, and R. W. Zimmerman, Comparison of methods for upscaling permeability from the pore scale to the core scale, *J. Hydraul. Res.*, (2004) **42**, 3-8.

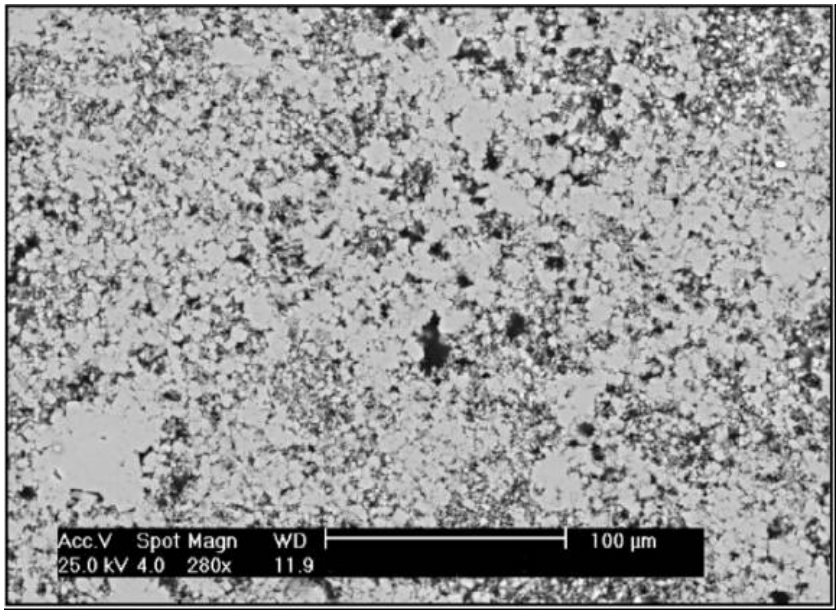

Figure 1: BSE image of carbonate sample A.

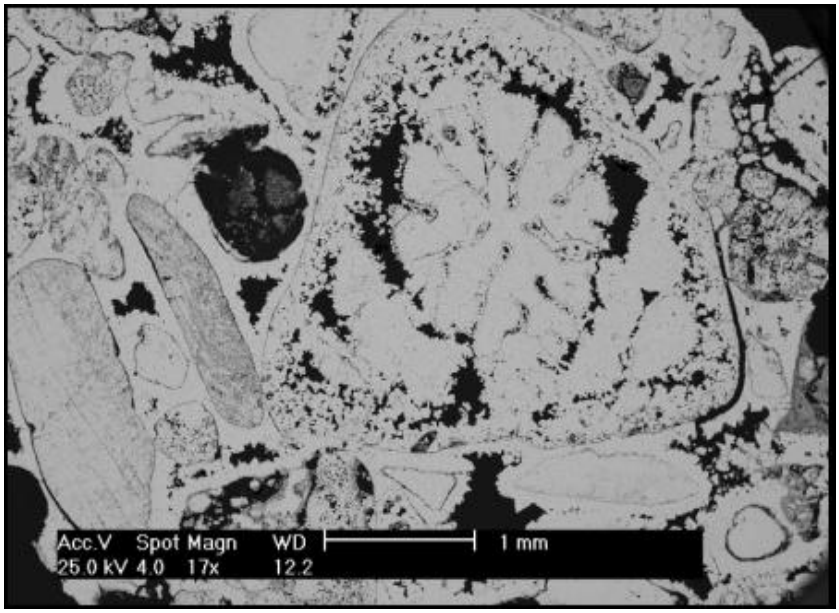

Figure 2: BSE image of carbonate sample D.

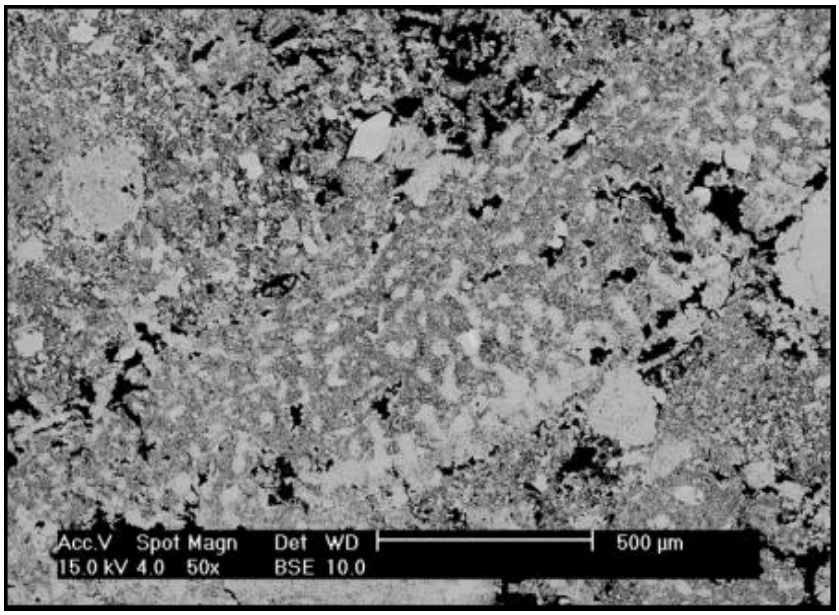

Figure 3: BSE image of carbonate sample E.

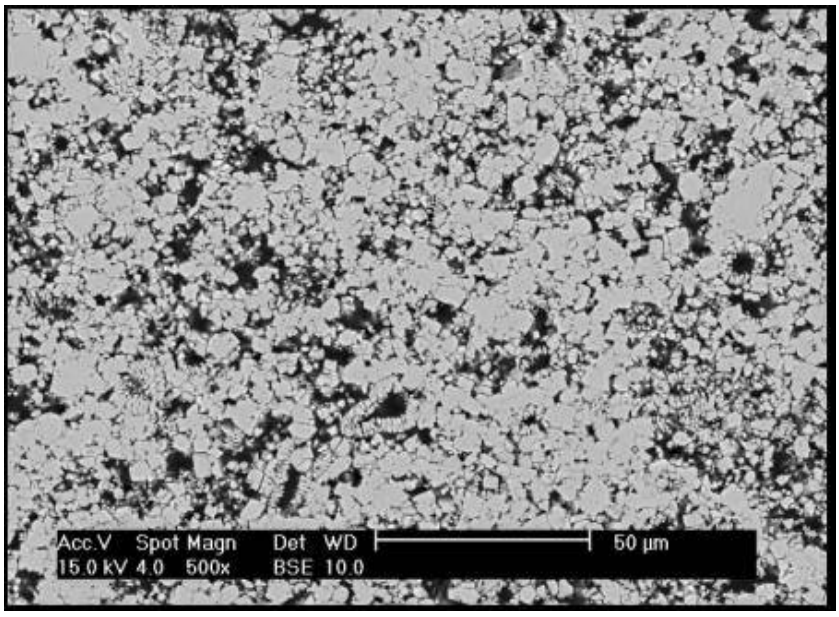

Figure 4: BSE image of carbonate sample F.